The Effect of Carbon Nanofiber on the Thermo-Physical Behavior of Polyethylene Oxide

A. R. Adhikari,[1] K. Lozano,[2] M. Chipara,[3] J. Qualls[4]

[1]*Department of Natural Sciences, Assumption College, 500 Salisbury St., Worcester, MA-01609*
[2]*Department of Mechanical Engineering, The University of Texas Pan American, Texas 78541*
[3]*Department of Physics and Geology, The University of Texas Pan American, Texas 78541*
[4]*Department of Physics and Astronomy, Sonoma State University, California 94928*

Received 5 February 2010; accepted 4 October 2010
DOI 10.1002/app.33542
Published online 14 February 2011 in Wiley Online Library (wileyonlinelibrary.com).

ABSTRACT: Composites of polyethylene oxide (PEO) filled with carbon nanofiber (CNF) were prepared using solution mixing followed by melt mixing. The morphology and thermophysical properties of these composites and of pristine polyethylene oxide were analyzed by scanning electron microscopy, differential scanning calorimetry, thermogravimetric analysis, and dynamical mechanical analysis. Crystallization kinetic data were analyzed within the Avrami approximation for the primary stage of crystallization. The influence of CNF on the temperature dependence crystallization of PEO and the tendency of forming three-dimensional crystallites at higher crystallization temperature were observed. The nucleation features of CNFs dispersed within PEO were investigated by using Lauritzen-Hoffman nucleation theory. Crystallization activation energies were also computed; the results are in agreement with the Lauritzen–Hoffman theory. Thermogravimetric analysis and dynamical mechanical analysis showed a gradual increase of the thermal stability and of the storage modulus of the polymeric matrix due to the loading with CNFs and formation of a polymer–carbon nanofiber interface.
 J Appl Polym Sci 120: 3574–3580, 2011

Key words: nanocomposites; differential scanning calorimetry; thermogravimetric analysis; carbon nanofiber; crystallization

INTRODUCTION

The dispersion of nanometer-sized fillers within polymeric matrices improves their physical properties (mechanical properties such as tensile strength and Young modulus and the thermal stability) and eventually adds new physical properties (such as antistatic features, electrical conductivity, or thermal conductivity). Various organic and inorganic fillers have been studied for this purpose and have resulted in composites with improved or new properties (controlled electrical resistivity, better stiffness, enhanced strength, and improved thermal stability).[1–5] Traditionally, reinforcement of polymers can be done with fillers of any sizes (macro to nano). However, nanometer-sized fillers expose (at the same loading fraction) a significantly larger surface and consequently allow for an increased fraction of macromolecular chains interacting with the filler and building the so-called polymer–filler interface. The outcome is an outstanding enhancement of mechanical, thermal, and electric features of the polymeric matrix due to the intrinsic features of carbon nanofibers (CNFs).[6] The high aspect ratio of these fillers triggered special interest particularly in the area of structural enhancement.[7,8] However, the potential of significant structural enhancements using different nanomaterials has remained elusive due to the technical difficulties achieving a good dispersion of the nanofiller and relatively weak and complex interactions between macromolecular chains and fillers.

Polyethylene oxide (PEO) is a semicrystalline thermoplastic polymer (a member of polyepoxides). The versatile nature of this polymer is that it is soluble in both aqueous and organic solvents[9] and has been extensively studied both experimentally[10,11] and theoretically.[12,13] The use of nanomaterials as reinforcement in PEO has shown promising applications. Yang et al.[14] studied the effects of phenoxy grafted MWNTs on the mechanical behavior of PEO-MWNT composites. They observed improvement in mechanical behavior such as an increase in tensile strength and Young modulus by 442 and 228%, respectively, with the expense of toughness at an optimum nanotube content of 1.5 wt %. Similarly, Ratna et al.[15] reported the thermomechanical properties of polyethylene oxide/clay nanocomposite. They

Correspondence to: M. Chipara (mchipara@utpa.edu).
Contract grant sponsor: NSF PREM; contract grant number: DMR 0934157.

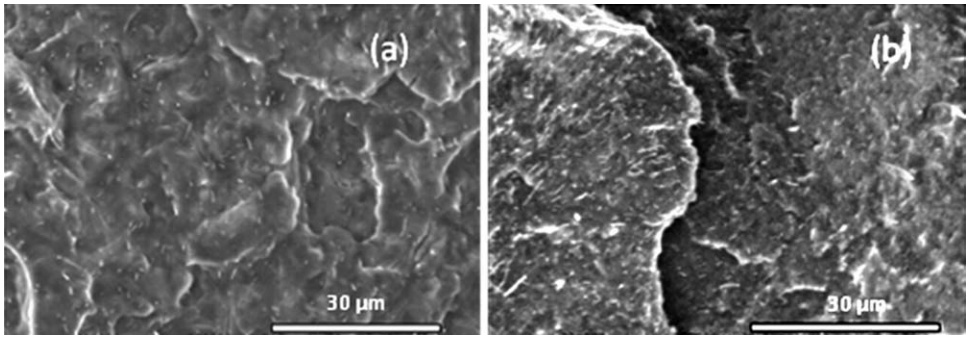

Figure 1 SEM images of PEO-CNF composite with (a) 1 wt % CNF and (b) 10 wt % CNF.

demonstrated an increase in tensile properties for clay contents up to 12.5 wt %. Crystallinity of the composites, however, decreased with the addition of clay.

The incorporation of nanomaterials into polymeric matrices affects the local structure of the polymeric system. Changes in crystal growth morphology and crystallization kinetics are expected and these could be highly dependent on processing methodologies that could significantly alter the ultimate material properties of semicrystalline polymers. In addition, additives in polymers have shown effective to alter the crystallization behavior. This article studies the effects of carbon nanofiber on the crystallization kinetics, mechanical behavior, and thermostability of PEO-CNF composites.

EXPERIMENTAL

Materials

The powder form of PEO ($(-CH_2CH_2O-)_n$) was purchased from Sigma-Aldrich. Average molecular weight of PEO is 100,000 with T_g and T_m at -67°C and 65°C, respectively. CNFs[16] (Pyrograph III PR-19- were kindly supplied by Applied Sciences) with diameter ranging from 100 to 200 nm and length from 30 to 100 μm have been used. CNFs were purified as described elsewhere.[17] Blends containing 1, 5, and 10 wt % CNFs dispersed in PEO were prepared using a two-step process, solution casting in chloroform followed by melt blending using a Haake Rheomix Polylab from Thermo Electron Corp. The suspension of CNF and the solution of PEO in chloroform were first prepared separately and then mixed. The mixtures after 1 h of ultrasonication were kept in air for 2 days to allow for solvent's evaporation. The resulted solid was then mixed in HAAKE minilab from Thermoelectron Corp. in two connected steps. The first at 90°C and 100 rotations per minute (rpm) for 6 min, followed by a 9-min mixing at 100°C with and 140 rpm. Finally, the mixtures were hot pressed using 11 MT load via a hydraulic press from Carver Inc. (Model No. 3912) at 100°C, for about 1 min. The reference sample was also prepared using the same procedure. The representative morphology of the obtained composites is shown in Figure 1. This shows that the dispersion of CNF in PEO is uniform.

Experimental techniques

Thermal analysis was carried out using TA instruments (TGA Q500 and DSC Q100). Thermogravimetric analysis (TGA) was performed by heating the sample ($\sim$ 10 mg) in a nitrogen atmosphere at a rate of 10°C/min from 50 to 600°C. Crystallization processes were studied using differential scanning calorimetry (DSC) under isothermal conditions. Indium was used for temperature calibration (T_m = 156.6 8°C, ΔH_m = 28.4 J/g). The samples were first heated to 120°C and held at this temperature for 30 min to erase any thermal history, and then cooled at 25°C/min to designated crystallization temperatures. DMA equipment (TA instrument DMA Q800) was used to study the mechanical behavior. Experiments were performed in tension mode over a temperature range of 40–90°C at a rate of 5°C/min and at a frequency of 1 Hz. The strain amplitude was 0.1% with a preload force of 0.01*N*. The data were analyzed for storage modulus. Surface images of the PEO and PEO-CNF composites were generated using a Hitachi *S*-3000*N* Scanning Electron Microscope (SEM).

RESULTS AND DISCUSSION

Crystallization

Isothermal crystallization analysis

Isothermal crystallization using DSC was carried out at four different crystallization temperatures 50, 51, 52, and 53°C, respectively. Figure 2(a) plots the isotherm of the first isothermal crystallization peaks for PEO and PEO-CNF composites at 50°C. Similar dependencies were noticed at 51, 52, and 53°C. Isotherm indicates sharp peak shift towards longer time at higher crystallization temperature. This demonstrates the sensitive crystallization behavior of PEO for a small change in crystallization temperature (T_{Cr}). This characteristic is more pronounced for

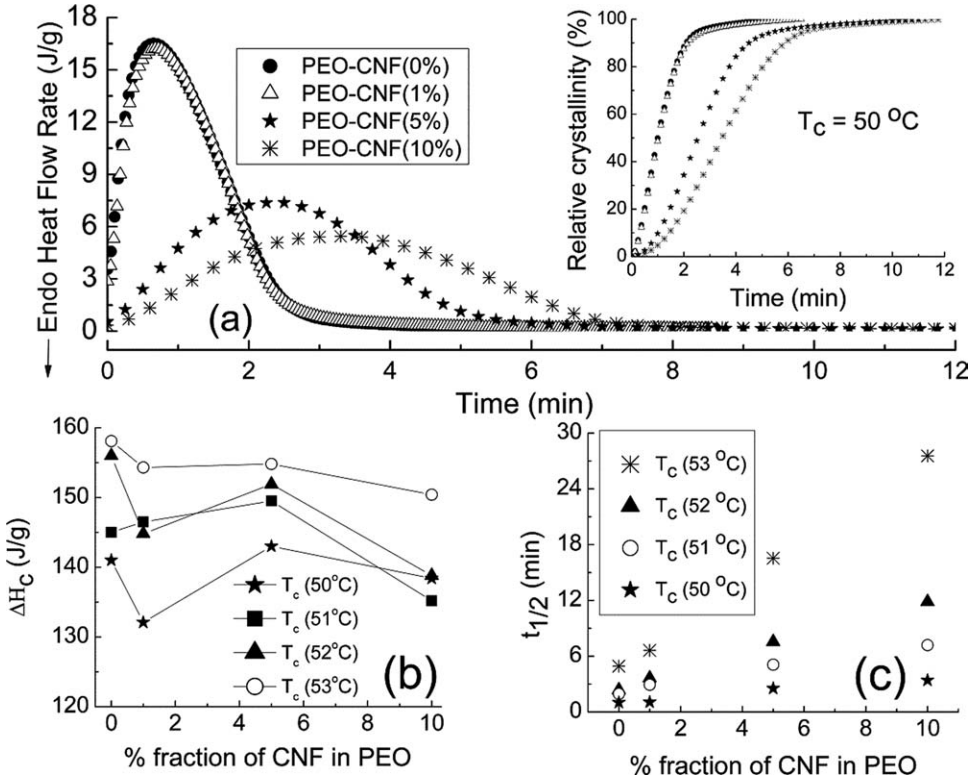

Figure 2 (a) Isothermal crystallization of PEO and PEO-CNF composites at 50°C (b). Effect of CNF on the crystallization half-time (c). As measured heat of crystallization as a function of weight fraction of CNF in PEO.

composites with higher filler loadings. The relative crystallization degree for crystalline fraction of PEO at any time during this process can be calculated by dividing the area at time (t) to the total area under crystallization. The crystallization degree for PEO has been obtained by dividing the total (integrated) area to the mass of the sample and to 194 J/g, which is the heat enthalpy for pure, 100% crystalline PEO. In the case of PEO-CNF composites, the mass of the sample has been corrected to reflect that solely the polymer undergoes crystallization. However, taking into account that the density of CNF is close to the density of the polymeric matrix, no density corrections were included in the calculation of the polymerization degree. The inset plot [Fig. 2(a)] shows the relative degree of crystallinity at a given time (defined for each sample as the ratio between the area calculated from the beginning of the crystallization up to that instant and the total area of the crystallization curve) as a function of crystallization time, for all samples. The total area under the crystallization curve, i.e., the heat enthalpy of the crystallization process has been carefully estimated. For pristine PEO a degree of crystallinity of 80% ± 5% has been obtained. The calculated heat enthalpy for PEO-CNF showed a weak decrease as the polymeric matrix is loaded with CNF. However, after correcting the data for the presence of CNFs we have concluded that within the experimental errors the degree of crystallinity of PEO is not affected by the presence of the filler (CNF). The changes observed in Figure 2(b) reflect just the fact that solely the polymer is subjected to crystallization and not the filler. Consequently, up to a multiplicative factor of about 0.8, the relative degree of crystallinity coincides to the actual degree of crystallinity for all samples.

Another parameter characteristic to the crystallization process is the half-time of crystallization ($t_{1/2}$) that can be extracted from these thermograms [Fig. 2(c)]. For all samples, $t_{1/2}$ increases with T_{Cr}. Shorter $t_{1/2}$ corresponds to higher crystallization rates. From Figure 2(f), it is observed that $t_{1/2}$ increases as the weight fraction of CNFs dispersed within PEO is increased. Such an increase is noticed even for the composite with 1 wt % CNF. This indicates that CNF leads to slower crystallization of PEO at all loadings.

Analysis based on Avrami equation

The isothermal crystallization process is described by the Avrami's theory[18]:

$$1 - X_c(t) = \exp(-Kt^n) \tag{1}$$

where $X_c(t)$ is the weight fraction of crystallized material at time t, K is a crystallization rate constant,

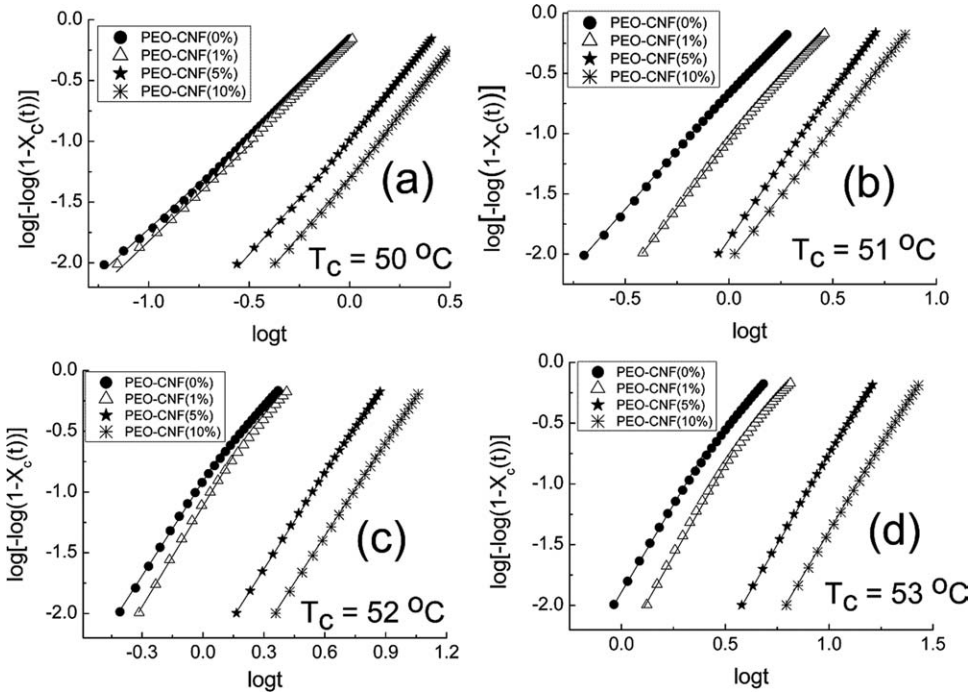

Figure 3 Avrami plot of $\log[-\log(1 - X_t)]$ versus $\log t$ for PEO-CNF composites at different crystallization temperatures (a) 50°C, (b) 51°C, (c) 52°C, and (d) 53°C. Note: Shown plots consist of 1–50% crystallinity of which 1–30% was fitted for kinetic parameters.

t is the crystallization time, and n is the Avrami exponent. The value of K and n depends on the crystalline morphology, growth rate, and the nature of nucleation process.[19] Double logarithm of eq. (1) gives,

$$\log[-\log(1 - X_c(t))] = \log K + n \log t \qquad (2)$$

The value of K and n can be extracted from the slope and intercept of resulting straight line when plotted $\log[-\log(1 - X_t)]$ versus $\log t$. In general, crystallization proceeds with primary crystallization followed by combined primary and secondary crystallization processes; the secondary crystallization is due to the impingement of spherulites and occurs in the later stage of crystallization.[20] Similar deviations at long crystallization times—indicating the presence of secondary crystallization—were observed in both pristine PEO and PEO-CNF composites. This study focuses on the analysis of the early stage of crystallization (with degree of crystallinity $\leq$ 30%). Figure 3 shows the Avrami plots for various PEO-CNF composites at different crystallization temperatures. The least square fit using eq. (2) in this crystallization step provides the value of kinetic parameters, K and n.

The values of K and n showed apparent dependency on crystallization temperature and weight content of CNF (see Fig. 4). The addition of CNF decreases the K values for all composites in all studied crystallization temperatures. The decrease is sharp at lower crystallization temperatures. These results substantiate $t_{1/2}$ results [Fig. 2(f)] and demonstrate the slower crystallization process. Further, the Avrami exponent showed sensitivity to the crystallization temperature. This is a typical nucleation controlled crystallization mechanism.[20] The Avrami parameter ranges from 1.5 to 3 depending on the crystallization temperature and the CNF content. At $T_{Cr} = 50$°C, n value for neat PEO is nearly equal to 1.5. This could be the average value of type and dimension of crystal growth. According to Avrami theory, this is considered a heterogeneous athermal nucleation resulting in one-dimensional crystal growth. This value slowly increases to about 2 resulting in 2D lamellar crystal growth and subsequently to about 3 when crystallized at $T_c = 53$°C, indicating the formation of spherulites. This shows that the crystallization is strongly dependent on crystallization temperature and changes from is one-dimensional needle-like, to two-dimensional circular, and to three-dimensional spherulites as crystallization temperature increases. The addition of CNF increases the n values even with 1 wt % CNF. Higher weight fractions of CNF have shown mixed influence with crystallization temperature. In other words, at lower T_{Cr} (50 and 51°C) n increases slowly with the CNF content, whereas n increases and levels off for all CNF contents at higher T_c (52 and 53°C).

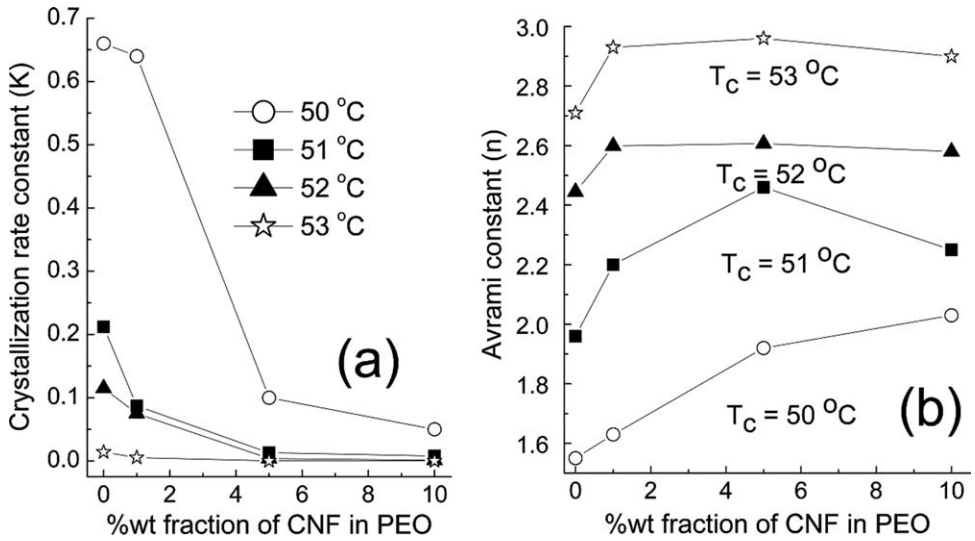

Figure 4 Plot of kinetic parameters during primary crystallization; rate constant (a) and Avrami exponent (b) as a function of weight fraction of CNF in PEO at different crystallization temperature.

Crystal growth rate

Crystal nucleation activity during isothermal crystallization is described by Lauritzen-Hoffman (LH) nucleation theory.[21] According to this theory, the dependence of crystal growth rate (G) with the crystallization temperature (T_c) is given by the following equation:

$$G = G_0 \exp\left[-\frac{U^*}{R(T_c - T_\infty)}\right] \exp\left[-\frac{K_g}{T_c(T_m^0 - T_c)}\right] \qquad (3)$$

where, G_o is a pre-exponential factor, U^* and T_∞ are the Vogel-Fulcher-Tamman-Hesse (VFTH) parameters that describe the transport of polymer across liquid/crystal interface, R is the gas constant, $\Delta T = (T_m^0 - T_c)$ is the degree of supercooling, T_m^0 is the melting temperature, and K_g is a nucleation constant. The values of U^* and T_∞ remain constant when crystallized at a temperature well above the glass transition temperature (T_g) of the polymer. The commonly used values of VFTH are values reported by Suzuki and Kovaces[22] ($U^* = 1500$ Cal/mol and $T_\infty = T_g - 30$ K and were used in this work) and Williams et al.[23] values ($U^* = 4120$ Cal/mol and $T_\infty = T_g - 51.6$ K). Based on eq. (3), the value of K_g can be extracted from the plot of lnG $+ U^*/R(T_c - T_\infty)$ versus $1/T_c\,\Delta T$ using an approximation[24]: $G \approx 1/t_{1/2}$. It can be seen that a straight-line fit is the best fit for all samples [Fig. 5(a)], indicating similar crystallization regime. Figure 5(b) plots the value of K_g obtained as a function of CNF content. Addition of CNF shows a clear increase of K_g. This shows that addition of CNF increases the work needed to create a new surface required for the crystallization.

Crystallization activation energy (ΔE)

Arrhenius equation describes the isothermal crystallization behavior as the process is thermally activated. Crystallization rate parameter (K) based on Arrhenius equation is given by;

$$K^{\frac{1}{n}} = k_0 \exp\left(-\frac{\Delta E}{RT_c}\right) \qquad (4)$$

$$\frac{\log K}{n} = \log k_0 - \frac{\Delta E}{RT_c} \qquad (5)$$

where k_o is the temperature independent pre-exponential factor, R is gas constant, and ΔE is activation energy. ΔE can be obtained from the slope of straight line resulting from eq. (5). The obtained activation energy of neat PEO and PEO-CNF composites

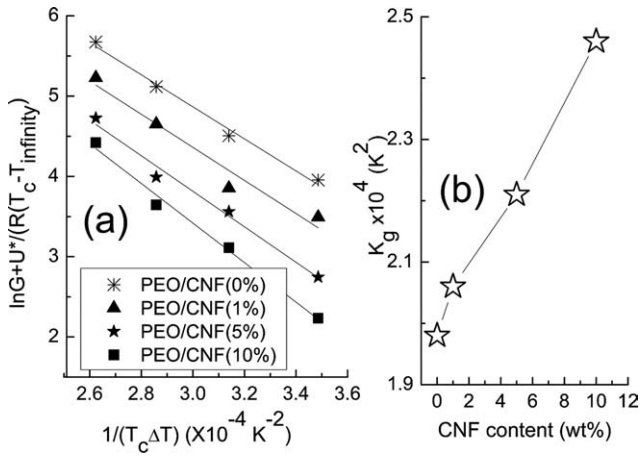

Figure 5 (a) Lauritzen-Hoffman plot for crystallization of PEO-CNF composites and (b) the variation of K_g with CNF content in PEO.

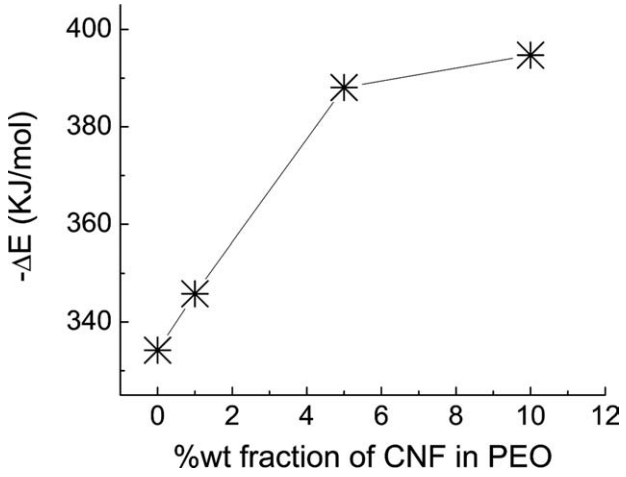

Figure 6 Variation of activation energy of PEO and PEO-CNF composites as a function of weight fraction of CNF in PEO.

is plotted in Figure 6. The system has to release energy while going to ordered state from the molten state, thus the ΔE values are negative. In this study, ΔE increased for all CNF content in correlation with the value of nucleation constant based on LH theory, the value of $t_{1/2}$ and the rate constant.

TGA analysis

Figure 7 illustrates the TGA thermogram of the as received PEO in nitrogen ambient. PEO is thermally stable up to 200°C and begins to lose weight gradually reaching maximum rate of degradation at a temperature (T_{max}) of 394°C. Similar decomposition kinetics was monitored for PEO composites with various amounts of CNF. As shown in Figure 7 inset, the addition of 1 wt % CNF increases the thermal stability of PEO value as observed by the

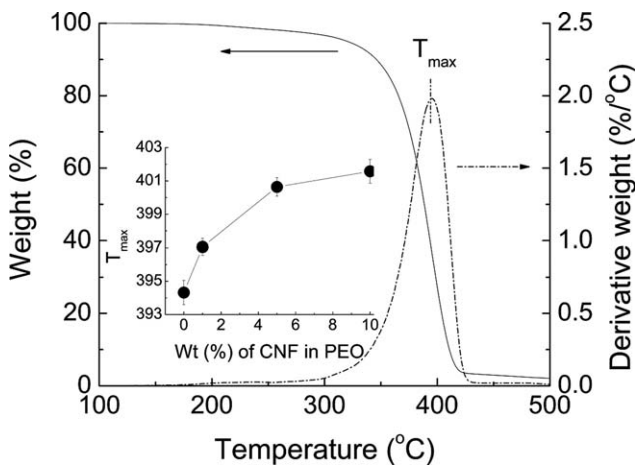

Figure 7 TGA (solid line) and DTA (dotted line) curves of as received polyethylene oxide in nitrogen environment. Inset Figure corresponds to the change of T_{max} with various weight fraction of CNF in PEO.

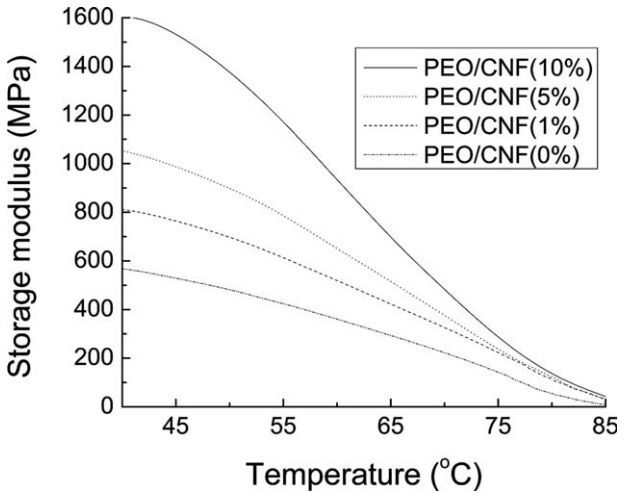

Figure 8 Storage modulus versus temperature of PEO-CNF composites at a frequency of 1 Hz.

increase of T_{max} by about 3°C. The thermal stability is further increased as the loading with CNFs increases. This reflects the interactions between PEO's chains and CNFs revealing the formation of a more stable interface.

DMA analysis

The result from the dynamical mechanical analyses can be utilized to mirror the thermal stability behavior of the composites. Figure 8 shows the temperature dependence of storage modulus taken from 40 to 90°C. The results show significant increases in mechanical behavior as a function of CNF loadings. For comparison, the storage modulus of 1, 5, and 10% PEO/CNF composites at room temperature increases by 42, 85, and 183% respectively, as compared to neat PEO. This behavior can be explained as follows. The polymer composites consist of two regions, one corresponds to pure polymer and the other is the interface region formed between filler and polymer. The types of interaction (chemical or physical) in the interphase depend upon the types of filler and polymer matrix. With the increase of CNF content, more and more surface area is available to interact with nearby polymer. This increases the interaction and the volume of interphase region. The increase of the storage modulus of PEO-CNF can be considered as due to larger interphase and stronger interaction between CNF and PEO with the increase of CNF content. From the DSC analysis, it is observed that crystallization behavior is strongly temperature dependent.

CONCLUSIONS

PEO-CNF composites have been prepared using a combined process of solution mixing and melt

mixing. SEM micrograph shows uniformly distributed CNF within the polymer. Although the final degree of crystallization of the polymeric component in PEO-CNF nanocomposites is not affected by the addiction of CNF, the nanofiller has an important effect on the crystallization kinetics and mechanism. Crystallization data in the primary stage were accurately fitted with the Avrami equation. The Avrami exponent of the neat PEO (at crystallization temperature 50°C) is about 1.5 indicating an 1D crystal growth. The crystallization mechanism of PEO geared towards 3D at higher crystallization temperature. This trend is observed for all composites. The exponential decrease of nucleation rate constant and decrease of nuclear activity based on LH theory with the CNF weight fraction demonstrates the slower crystallization process of PEO with the addition of CNF. This observation is corroborated from the observed higher activation energy for the transport of the polymer with the content of CNF. These results suggest that the crystallization process is not ignited at the interface PEO-CNF but rather within the core of the polymeric phase. Crystallites are growing towards the filler and eventually nucleating within the interface. The collisions between macromolecular chains and nanofiller does not allow the macromolecular chains to reach the equilibrium positions, and consequently to fold into crystalline domains. Detailed studies are necessary to determine the role of the interface in the crystallization process.

Small deviation in temperature (1°C) values has significantly changed the values of $t_{1/2}$ and kinetic parameters (n and K). This demonstrates the impact that the processing parameter (temperature in this case) could have on the nano-micro structure of PEO-CNF composites and ultimately on the resulting macro-properties. Processing parameters effects need to be well understood before these nano-reinforced composites are brought to practical applications. Thermal stability of PEO was enhanced with the addition of CNFs due to the formation of a polymer–filler interface. Thermal stability behavior was corroborated with DMA results. These results demonstrate that CNF could effectively reinforce PEO.

References

1. Wen, J.; Wilkes, G. L. Chem Mater 1996, 8, 1667.
2. Chang, J. H.; An, Y. U. J Polym Sci B: Polym Phys 2002, 40, 670.
3. Leroux, F. J Nanosci Nanotech 2006, 6, 303.
4. Okamoto, M. Mater Sci Tech 2006, 22, 756.
5. Patel, S.; Bandyopadhyay, A.; Vijayabaskar, V.; Bhowmick, A. K. J Mater Sci 2006, 41, 927.
6. Dressaulhaus, M. S.; Dressaulhaus, G.; Charlier, J. C.; Hernandez, E. Philos Trans R Soc Lond A 2004, 362, 2065.
7. Magaraphan, R.; Lilayuthalert, W.; Sirivat, A.; Schwank, J. W. Compos Sci Tech 2001, 61, 1253.
8. Wu, C. L.; Zhang, M. Q.; Rong, M. Z.; Friedrich, K. Compos Sci Technol 2002, 62, 1327.
9. Brandrup, J.; Immergut, E. H.; Eds. Polymer Handbook, 2nd ed.; Wiley: New York, 1974.
10. Chen-Yang, Y. W.; Wang, Y. L.; Chen, Y. T.; Li, Y. K.; Chen, H. C.; Chiu, H. Y. J Power Sources 2008, 182, 340.
11. Tan, J.; Brash, J. L. J Biomed Mater Res Part A 2008, 85, 862.
12. Aray, Y.; Marquez, M.; Rodriguez, J.; Vega, D.; Simon-Manso, Y.; Coll, S.; Gonzalez, C.; Weitz, D. A. J Phys Chem B 2004, 108, 2418.
13. Dormidontova, E. E. Macromolecules 2002, 35, 987.
14. Yang, B. X.; Shi, J. H.; Pramoda, K. P.; Goh, S. H. Nanotechnology 2007, 18, 125606.
15. Ratna, D.; Divekar, S.; Samui, A. B.; Chakraborty, B. C.; Banthia, A. K. Polymer 2006, 47, 4068.
16. Joshi, M.; Butola, B. S. Polymer 2004, 45, 4953.
17. Lozano, K.; Files, B.; Rodrigues-Macias, F.; Barrera, E. V. Symposium Powder Materials: Current Research and Industrial Practices; TMS Fall Meeting, Cincinnati OH, USA, 1999; p 333.
18. Avrami, M. J Chem Phys 1940, 8, 212.
19. Wunderlich, B.Macromolecular Physics; Academic Press: New York, 1976.
20. Madelkern, L. Crystallization of Polymers; McGrow-Hill: New York, 1964.
21. Hoffman, J. D.; Davis, G. T.; Lauritzen, J. I., Jr. In Treatise on Solid State Chemistry; Hannay, N. B., Ed.; Plenum Press: New York, 1976; Vol. 3.
22. Suzuki, T.; Kovacs, A. J. Polym J 1970, 1, 82.
23. Williams, M. L.; Landel, R. F.; Ferry, J. D. J Am Chem Soc 1955, 77, 3701.
24. Mucha, M.; Krolikowski, Z. J Therm Anal Cal 2003, 74, 549.